JACC: CARDIOVASCULAR IMAGING VOL. ■, NO. ■, 2018

PUBLISHED BY ELSEVIER

Cardiac Structural and Functional Consequences of Amyloid Deposition by Cardiac Magnetic Resonance and Echocardiography and Their Prognostic Roles

Daniel S. Knight, MBBS, MD(Res),[a] Giulia Zumbo, MD,[a] William Barcella, PhD,[b] Jennifer A. Steeden, M.Eng, PhD,[c] Vivek Muthurangu, MD,[c] Ana Martinez-Naharro, MD,[a] Thomas A. Treibel, MBBS,[d] Amna Abdel-Gadir, MBBS,[d] Heerajnarain Bulluck, MBBS, PhD,[e] Tushar Kotecha, MBChB,[a] Rohin Francis, MBBS,[a] Tamer Rezk, MBBS,[a] Candida C. Quarta, MD, PhD,[a] Carol J. Whelan, MD,[a] Helen J. Lachmann, MD,[a] Ashutosh D. Wechalekar, MD, PhD,[a] Julian D. Gillmore, MD, PhD,[a] James C. Moon, MD,[d] Philip N. Hawkins, PhD, FMedSci,[a] Marianna Fontana, MD, PhD[a]

ABSTRACT

OBJECTIVES This cross-sectional study aimed to describe the functional and structural cardiac abnormalities that occur across a spectrum of cardiac amyloidosis burden and to identify the strongest cardiac functional and structural prognostic predictors in amyloidosis using cardiac magnetic resonance (CMR) and echocardiography.

BACKGROUND Cardiac involvement in light chain and transthyretin amyloidosis is the main driver of prognosis and influences treatment strategies. Numerous measures of cardiac structure and function are assessed by multiple imaging modalities in amyloidosis.

METHODS Three hundred twenty-two subjects (311 systemic amyloidosis and 11 transthyretin gene mutation carriers) underwent comprehensive CMR and transthoracic echocardiography. The probabilities of 11 commonly measured structural and functional cardiac parameters being abnormal with increasing cardiac amyloidosis burden were evaluated. Cardiac amyloidosis burden was quantified using CMR-derived extracellular volume. The prognostic capacities of these parameters to predict death in amyloidosis were assessed using Cox proportional hazards models.

RESULTS Left ventricular mass and mitral annular plane systolic excursion by CMR along with strain and E/e' by echocardiography have high probabilities of being abnormal at low cardiac amyloid burden. Reductions in biventricular ejection fractions and elevations in biatrial areas occur at high burdens of infiltration. The probabilities of indexed stroke volume, myocardial contraction fraction, and tricuspid annular plane systolic excursion (TAPSE) being abnormal occur more gradually with increasing extracellular volume. Ninety patients (28%) died during a median follow-up of 22 months (interquartile range: 10 to 38 months). Univariable analysis showed that all imaging markers studied significantly predicted outcome. Multivariable analysis showed that TAPSE (hazard ratio: 1.46; 95% confidence interval: 1.16 to 1.85; $p < 0.01$) and indexed stroke volume (hazard ratio: 1.24; 95% confidence interval: 1.04 to 1.48; $p < 0.05$) by CMR were the only independent predictors of mortality.

CONCLUSIONS Specific functional and structural abnormalities characterize different burdens of cardiac amyloid deposition. In a multimodality imaging assessment of a large cohort of amyloidosis patients, CMR-derived TAPSE and indexed stroke volume are the strongest prognostic cardiac functional markers. (J Am Coll Cardiol Img 2018;■:■–■)

From the [a]National Amyloidosis Centre, University College London, Royal Free Hospital, London, United Kingdom; [b]Department of Statistical Science, University College London, United Kingdom; [c]Centre for Cardiovascular Imaging, Institute of Cardiovascular Science, University College London and Great Ormond Street Hospital for Children, London, United Kingdom; [d]Barts Heart Centre, St. Bartholomew's Hospital, London, United Kingdom; and [e]The Hatter Cardiovascular Institute, Institute of Cardiovascular Science, University College London, United Kingdom. The authors have reported that they have no relationships relevant to the contents of this paper to disclose. Drs. Knight and Zumbo contributed equally to this work and are joint first authors.

Manuscript received April 19, 2017; revised manuscript received February 12, 2018, accepted February 15, 2018.

ISSN 1936-878X/$36.00 https://doi.org/10.1016/j.jcmg.2018.02.016

ABBREVIATIONS AND ACRONYMS

AL = light-chain amyloidosis

ATTR = transthyretin-related amyloidosis

CMR = cardiac magnetic resonance

ECV = extracellular volume

EF = ejection fraction

LA = left atrial

LGE = late gadolinium enhancement

LGS = longitudinal global strain

LV = left ventricular

MAPSE = mitral annular plane systolic excursion

MCF = myocardial contraction fraction

RA = right atrial

RV = right ventricular

SV = stroke volume

TAPSE = tricuspid annular plane systolic excursion

Systemic amyloidosis is a fatal disease caused by the progressive deposition of abnormal insoluble protein fibrils in the extracellular space, leading to the loss of normal tissue architecture and function (1). Cardiac amyloidosis is due to intramyocardial amyloid infiltration, which leads to progressive structural and functional changes (2,3). The most frequent types of systemic amyloidosis associated with clinically relevant cardiac involvement are light-chain amyloidosis (AL) due to a clonal plasma cell dyscrasia, which produces the immunoglobulin light chains of the fibrillary deposits; hereditary, transthyretin (TTR)-related form (ATTRm), which can be caused by more than 100 mutations of TTR, a transport protein mainly synthesized by the liver; and wild-type (non-mutant) TTR-related amyloidosis (ATTRwt), which mainly affects the hearts of elderly men (1).

Cardiac involvement in both AL and ATTR amyloidosis is the main predictor of mortality and influences therapeutic choices (4,5). Late gadolinium enhancement (LGE) and extracellular volume (ECV) assessment by cardiac magnetic resonance (CMR) are known to be diagnostic and prognostic in cardiac amyloidosis (2). Echocardiography and CMR are both commonly used imaging modalities to assess cardiac amyloidosis that generate a plethora of functional and structural metrics aside from tissue characterization parameters. Many of these cardiac functional and structural parameters show prognostic value when studied in isolation (3,6-12). However, their relative prognostic importance and their behavior in the natural history of cardiac infiltration have never been investigated.

The aims of this study were to describe the functional and structural cardiac abnormalities that occur across a spectrum of cardiac amyloid burden in AL and ATTR cardiac amyloidosis, and to identify the strongest cardiac functional predictors of prognosis in systemic amyloidosis.

METHODS

AMYLOIDOSIS PATIENTS. Subjects were recruited at the National Amyloidosis Centre, Royal Free Hospital, London, United Kingdom, from 2010 to 2015. A retrospective, cross-sectional analysis of 433 patients who underwent CMR and echocardiography was performed. Patients with datasets not containing all of the structural and functional cardiac metrics selected for analysis in this study were excluded. The remaining 322 patients were categorized into 3 groups:

1. Subjects with AL amyloidosis: 133 patients with biopsy-proven systemic AL amyloid (86 men, 65%; age 66 [range 57 to 71] years), with biopsy specimens from the myocardium (n = 7, 5%) or other tissues (n = 126, 95%).
2. Subjects with ATTR amyloidosis: 158 patients (139 men, 88%; age 74 ± 8 years) with cardiac ATTR amyloidosis and 20 with suspected cardiac ATTR amyloidosis (12 men, 60%; age 70 ± 15 years) were recruited. The definitions of definite and suspected cardiac ATTR amyloidosis have been previously described (13,14). To summarize, cardiac ATTR amyloidosis was defined as the combination of symptoms with an echocardiogram consistent with or suggestive of cardiac amyloidosis, grade 2 or 3 cardiac uptake on the technetium 99m (^{99m}Tc)-labeled 3,3-diphosphono-1,2-propanodicarboxylic acid (^{99m}Tc-DPD) scintigraphy in the absence of a monoclonal gammopathy or, in the presence of monoclonal gammopathy, a cardiac biopsy positive for TTR. Suspected cardiac ATTR amyloidosis was defined by grade 1 cardiac uptake on ^{99m}Tc-DPD in the absence of monoclonal gammopathy. Seventy-two percent (n = 128) of patients with ATTR amyloidosis had histologic proof of ATTR amyloidosis by Congo red and immunohistochemical staining of myocardial (n = 40, 22%) or other tissues (n = 88, 49%). All subjects underwent sequencing of exons 2, 3, and 4 of the *TTR* gene.
3. TTR gene mutation carriers: In addition, there were 11 subjects with amyloidogenic *TTR* gene mutations (4 men, 36%; age 46 ± 8 years) defined as individuals with no evidence of clinical disease (including no cardiac uptake on ^{99m}Tc-DPD scintigraphy and normal echocardiography, CMR, N-terminal pro-brain natriuretic peptide and troponin T).

EXCLUSION CRITERIA. We excluded all patients with datasets not containing all of the structural and functional cardiac metrics selected for analysis. Patients with contraindications to CMR (such as CMR-incompatible devices) were excluded from the original study cohort. Patients with a glomerular filtration rate <30 ml/min underwent a noncontrast study protocol (n = 5) unless informed consent was obtained for a contrast study protocol for clinical diagnostic purposes (n = 4). All ethics were approved by the UCL/UCLH Joint Committees on the Ethics of Human Research Committee, and all participants provided written informed consent.

ECHOCARDIOGRAPHY ACQUISITION AND ANALYSIS. Echocardiographic assessments were performed using a Vivid E9 ultrasound machine (GE Healthcare, Milwaukee, Wisconsin). Image quality was optimized by adjusting probe frequency (range 1.7 to 2.0 MHz) and temporal resolution (60 to 120 frames/s). Left ventricular (LV) structure, systolic, and diastolic assessment was performed according to published recommendations (15–17). This included the analysis of multiple beats in atrial arrhythmia at the discretion of the clinical study operator. All echocardiography analysis was performed by investigators blinded to the CMR results. The echocardiographic functional parameters assessed in the multivariable model were E/e′ and apical 4-chamber longitudinal global strain (LGS). For the former measure, pulsed-wave tissue Doppler imaging of the septal and lateral mitral annuli in the 4-chamber view was performed to obtain peak early diastolic (e′) tissue velocities, with septal and lateral velocities averaged to obtain a mean value. The peak early diastolic transmitral inflow wave (E) was obtained by pulsed-wave Doppler imaging with the sample volume placed at the tips of the mitral valve in the apical 4-chamber view. Myocardial deformation was assessed using commercially available speckle-tracking software (EchoPac PC dimension software version 112, GE Healthcare). Between 2 to 3 cardiac cycles from an apical 4-chamber view were acquired with appropriate image optimization and digitally stored for offline analysis. The endocardium of the LV was manually traced from the medial and lateral mitral valve annuli and a region of interest (ROI) automatically generated to cover the LV myocardium. The ROIs were adjusted to optimize the tracking quality if needed.

CMR PROTOCOL. All participants underwent standard CMR on 1.5-T clinical scanners (either Avanto or Aera, Siemens Healthcare, Erlangen, Germany). A standard volume and LGE study was performed in all patients. Retrospectively gated balanced steady state free precession end-expiratory breath-hold cines were acquired covering the bases to apices of both ventricles in the short-axis for patients in sinus rhythm. Patients with atrial arrhythmia had a similarly planned short-axis biventricular stack of cine images acquired using either prospectively gated balanced steady state free precession cines or real-time cine imaging at the discretion of the clinical study operator. Slice thickness was 7 mm with a 3-mm slice gap. The gadolinium-based contrast agent used was 0.1 mmol/kg of gadoterate meglumine (gadolinium-DOTA, marketed as Dotarem, Guerbet SA, Paris, France) for LGE imaging as previously described (2). For native T1 mapping, basal and mid-ventricular short axis images and 4-chamber long-axis images were acquired using the shortened modified look-locker inversion recovery or modified look-locker inversion recovery sequences after regional shimming, as previously described (18).

CMR IMAGE ANALYSIS. All CMR images and maps were analyzed offline. All CMR analysis was performed by investigators blinded to the echocardiography results. Endocardial borders of both ventricles were manually traced at end-diastole and end-systole, the time points of which were identified by the largest and smallest cavity areas respectively. LV stroke volume (SV) was the difference between the LV end-diastolic volume (EDV) and LV end-systolic volume (ESV), and ejection fraction (EF) was calculated as: (SV/EDV) × 100. LV mass was calculated from the end-diastolic frames by manually tracing an epicardial contour. The papillary muscles and trabeculae were excluded from the blood pool by the endocardial contour (thus they were included when measuring mass and excluded when measuring cavity volumes). Annular plane systolic excursion for both the mitral annular plane systolic excursion (MAPSE) and tricuspid annular plane systolic excursion (TAPSE) was analyzed for the lateral valvular annulus. Maximal biatrial areas were manually traced at the ventricular end-systolic frames from a 4-chamber cine.

ECV was used as the primary measure of cardiac amyloidosis burden, and was calculated as previously described (19). To summarize, T1 values were obtained by drawing a single ROI in each of the 4 required areas: myocardial T1 estimates (basal to mid septum in 4-chamber map) and blood T1 estimates (LV cavity blood pool in 4-chamber map, avoiding the papillary muscles) before and after contrast administration. Hematocrit was obtained in all subjects immediately before each CMR study. ECV was calculated as: myocardial ECV = (1-hematocrit) × $(\Delta R1_{myocardium}/\Delta R1_{blood})$, where R1 = 1/T1.

STATISTICAL ANALYSIS. Statistical analysis was performed using SPSS version 24.0 (IBM Corporation, Armonk, New York) and R programming language (R Foundation for Statistical Computing, Vienna, Austria). Data were examined for normality using the Kolmogorov-Smirnov normality test. Descriptive statistics are expressed as mean ± SD when normally distributed and median (interquartile range) when non-normally distributed. Proportions are expressed as percentages. Systematic differences between measurements were evaluated with the Student's *t*-test (2-tailed) to compare parametric data, and the Mann-

TABLE 1 Main Clinical Characteristics and ECG Findings in Patients With AL and ATTR Amyloidosis

				ATTR Patients (n = 189)		
	All Patients (n = 322)	AL Patients (n = 133)	ATTR Patients (n = 189)	Definite (n = 158)	Suspected (n = 20)	Gene Mutation Carriers (n = 11)
Age, yrs	71 (63-77)	66 (57-71)*	74 (68-80)	75 (70-81)	74 (52-83)	45 (42-53)
Female	81 (25.2)	47 (35.3)*	34 (18.0)	19 (12)	8 (40)	7 (63.6)
Ethnicity						
White	267 (82.9)	120 (90.2)	147 (77.8)	119 (75.3)	17 (85.0)	11 (100)
Black	48 (14.9)	6 (4.5)*	42 (22.2)	39 (24.7)	3 (15)	0 (0)
Asian	5 (1.6)	5 (3.8)	0 (0)	0 (0)	0 (0)	0 (0)
Arab	1 (0.3)	1 (0.8)	0 (0)	0 (0)	0 (0)	0 (0)
Mixed	1 (0.3)	1 (0.8)	0 (0)	0 (0)	0 (0)	0 (0)
Clinical history of hypertension	63 (19.6)	27 (20.3)	36 (19.0)	32 (20.3)	3 (15.0)	1 (9.1)
eGFR, ml/min/1.73 m^2	67 (48-84)	75 (50-90)†	63 (47-79)	59 (45-73)	82 (62-89)	86 (76-100)
Systolic BP, mm Hg	120 (110-133)	121 (109-138)	120 (110-130)	119 (110-129)	128 (114-148)	121 (112-132)
Diastolic BP, mm Hg	72 (65-80)	72 (65-83)	71 (65-79)	71 (64-79)	70 (67-78)	75 (69-81)
NT-proBNP, pmol/l	220 (86-467)	170 (65-389)‡	280 (112-522)	322 (172-591)	27 (13-118)	7 (3-9)
6MWT, meters	330 ± 136	321 ± 127	335 ± 141	313 ± 133	374 ± 141	526 ± 60
Sinus rhythm	155 (48.1)	31 (23.3)*	124 (65.6)	96 (60.8)	18 (90.0)	10 (90.9)
Heart rate, beats/min	73 ± 13	78 ± 13*	69 ± 12	69 ± 13	71 ± 11	70 ± 12
PR, ms	184 (157-214)	168 (148-194)*	195 (162-224)	202 (184-232)	170 (153-195)	144 (130-154)
QRS, ms	102 (92-120)	98 (88-109)*	106 (94-132)	108 (96-146)	94 (88-112)	88 (84-92)
Sum limb leads voltage, mm	29 (21-39)	26 (19-36)‡	30 (23-39)	29 (21-39)	33 (26-52)	37 (30-38)
Sum chest leads voltage, mm	78 (62-100)	73 (57-93)†	82 (64-106)	84 (65-108)	69 (63-88)	72 (57-86)
Medications						
Beta-blocker	98 (30.4)	29 (21.8)*	69 (36.5)	67 (42.4)	2 (10.0)	0 (0)
Loop diuretic	183 (56.8)	54 (40.6)*	129 (68.3)	124 (78.5)	5 (25.0)	0 (0)
Aldosterone antagonist	76 (23.6)	17 (12.8)*	59 (31.2)	57 (36.1)	2 (10.0)	0 (0)
ACE inhibitor or angiotensin receptor blocker	117 (36.3)	36 (27.1)*	81 (42.9)	78 (49.4)	3 (15.0)	0 (0)

Values are median (Q1-Q3), n (%), or mean ± SD. *$p < 0.001$, †$p < 0.01$, and ‡$p < 0.05$, for AL versus ATTR amyloidosis patients.

6MWT = 6-min walk test; ACE = angiotensin converting enzyme; AL = light-chain amyloidosis; ATTR = transthyretin amyloidosis; BP = blood pressure; ECG = electrocardiogram; eGFR = estimated glomerular filtration rate; NT-proBNP = N-terminal pro-brain natriuretic peptide.

Whitney U test was used to compare nonparametric data. The chi-square test or Fisher exact test (2-sided) was used to compare proportions data as appropriate. Comparisons between groups were performed by 1-way analysis of variance for parametric data and by the Kruskal-Wallis 1-way analysis of variance for nonparametric data. Values of $p < 0.05$ were considered statistically significant.

Eleven functional and structural cardiac variables by echocardiography (E/e′, LGS) and CMR (indexed left atrial [LA] area, indexed LV mass, indexed right atrial [RA] area, indexed SV, LVEF, MAPSE, right ventricular [RV] EF, TAPSE, myocardial contraction fraction [MCF]) were selected a priori based upon clinical relevance. The focus of this study is on the effects of myocardial infiltration on cardiac structure and function, since the prognostic capacities of LGE and ECV assessment in cardiac amyloidosis are already well established (2). Therefore, the statistical analyses included only structural and functional cardiac imaging biomarkers (and no tissue characterization parameters) as the variables under investigation. Biventricular function and biatrial areas were assessed using CMR rather than echocardiography due to the superior accuracy and reproducibility of the former imaging modality for these purposes. MAPSE and TAPSE were also assessed by CMR on the same 4-chamber view as biatrial area measurements as per the standard clinical CMR protocol at our institution. The MCF, defined as the ratio of SV to myocardial volume, has been shown to be prognostic in cardiac amyloidosis (20). Simple logistic regression analysis was performed for evaluating the probability of the selected cardiac structural and functional parameters being abnormal across the spectrum of ECV. Cut-offs for defining abnormalities in these variables were chosen according to published reference guidelines: E/e′ >8 (21), indexed LA area >15 cm^2/m^2 (22), indexed RA area >16 cm^2/m^2 (22), LGS <-20% (23), LVEF <57% (22), RVEF <52% (22), indexed SV <42 ml/m^2 (22), indexed LV mass >81 g/m^2 (22), MAPSE < 11 mm, TAPSE <16 mm, and MCF <38% (24).

TABLE 2 CMR and Echocardiographic Findings in Patients With AL and ATTR Amyloidosis

	All Patients (n = 322)	AL Patients (n = 116)			ATTR Patients (n = 183)		
ECV measured by CMR							
ECV	0.56* (0.43-0.65)		0.45 (0.37-0.56)			0.61 (0.51-0.69)†	
ECV tertile		0.23-0.48 (n = 72, 62%)	0.49-0.61 (n = 31, 27%)	0.62-0.92 (n = 13, 11%)	0.23-0.48 (n = 35, 19%)	0.49-0.61 (n = 59, 32%)	0.62-0.92 (n = 89, 49%)
Echocardiography parameters							
IVSd, cm	1.5 (1.3-1.7)	1.2 (1.1-1.3)	1.4 (1.3-1.5)	1.6 (1.5-1.75)‡	1.1 (1.0-1.5)	1.6 (1.4-1.7)	1.7 (1.6-1.9)†
E wave, cm/s	0.81 (0.66-0.95)	0.76 (0.59-0.93)	0.90 (0.79-1.01)	0.82 (0.63-0.95)§	0.76 (0.65-0.87)	0.86 (0.74-1.02)	0.80 (0.69-0.95)§
A wave, cm/s	0.59 (0.37-0.78)	0.71 (0.59-0.88)	0.60 (0.41-0.82)	0.32 (0.21-0.75)‡	0.62 (0.55-0.81)	0.61 (0.38-0.74)	0.31 (0.25-0.46)†
E/A	1.35 (0.92-2.30)	0.93 (0.78-1.37)	1.53 (0.94-2.42)	1.61 (0.95-2.86)‡	1.16 (0.95-1.35)	1.50 (1.00-2.39)	2.48 (1.79-3.18)†
Average e', cm/s	0.06 (0.05-0.08)	0.07 (0.06-0.09)	0.06 (0.05-0.08)	0.04 (0.03-0.07)‡	0.08 (0.07-0.11)	0.05 (0.04-0.07)	0.05 (0.04-0.06)†
E/e'	14 (9-19)	10 (8-16)	15 (10-19)	21 (10-27)‡	9 (6-12)	15 (12-20)	17 (13-21)†
E-wave deceleration time, ms	181 (148-215)	200 (162-241)	180 (131-207)	166 (115-235)	195 (156-227)	185 (150-225)	165 (139-191)‡
Strain, %	13 (9-17)	18 (14-20)	12 (8-16)	9 (7-11)†	19 (17-20)	12 (10-15)	9 (7-11)†
CMR parameters							
$LVEDV_i$, ml/m^2	61 (52-70)	59 (52-67)	57 (45-62)	59 (48-67)	60 (50-70)	60 (51-73)	68 (59-80)‡
$LVESV_i$, ml/m^2	22 (16-32)	17 (13-23)	17 (11-25)	27 (20-33)‡	19 (12-22)	20 (16-33)	33 (25-43)†
$RVEDV_i$, ml/m^2	63 (54-76)	59 (51-67)	56 (49-65)	61 (52-67)	60 (53-70)	62 (53-76)	72 (63-89)†
$RVESV_i$, ml/m^2	25 (18-37)	19 (16-25)	21 (14-28)	26 (21-42)§	20 (16-26)	25 (18-30)	38 (31-50)†
LV SV_i, ml/m^2	37 ± 10	42 ± 8	36 ± 9	30 ± 9†	41 ± 8	38 ± 8	33 ± 9†
LVEF, %	63 (50-72)	71 (65-75)	68 (57-76)	57 (42-62)†	71 (64-77)	64 (56-71)	50 (40-58)†
RVEF, %	60 (49-68)	67 (60-73)	64 (52-71)	52 (36-57)†	66 (63-72)	60 (52-67)	47 (36-55)†
MAPSE, mm	8 (6-10)	10 (8-13)	7 (5-9)	4 (4-6)†	12 (10-13)	8 (6-9)	6 (5-8)†
TAPSE, mm	14 (10-19)	19 (14-22)	14 (9-20)	10 (8-14)†	20 (18-24)	14 (11-17)	11 (8-13)†
LV $mass_i$, g/m^2	109 (80-137)	79 (63-99)	96 (80-111)	122 (108-144)†	72 (60-95)	118 (102-139)	145 (124-167)†
LA $area_i$, cm^2/m^2	15 ± 4	13 ± 3	13 ± 4	15 ± 2§	13 ± 3	16 ± 3	17 ± 3†
RA $area_i$, cm^2/m^2	13 (10-16)	12 (10-14)	12 (10-14)	10 (9-15)	12 (10-13)	13 (11-15)	16 (14-19)†
RV LGE*	229 (77)	34/72 (47)	28/31 (90)	11/13 (85)†	13/35 (37)	57/59 (97)	86/89 (97)†
Precontrast T1, ms	1,089 (1,049-1,127)	1,046 (999-1,085)	1,135 (1,100-1175)	1164 (1,119-1,195)†	1003 (963-1,052)	1,086 (1,067-1,106)	1,115 (1,091-1,142)†
MCF, %	35.5 (25.4-54.9)	56.3 (42.9-71.4)	38.0 (30.1-51.8)	24.1 (19.8-33.3)†	62.2 (36.9-72.3)	34.2 (25.5-41.3)	24.2 (19.4-28.3)†

Values are median (Q1-Q3) or mean ± SD. *Excluding <23 patients who did not have ECV measured. †$p < 0.001$, ‡$p < 0.01$, and §$p < 0.05$ for the distribution of variables across ECV tertiles in the AL and ATTR patient cohorts.

CMR = cardiac magnetic resonance; ECV = extracellular volume; IVSd = interventricular septum thickness in diastole; LA $area_i$ = left atrial area indexed; LGE = late gadolinium enhancement; LV = left ventricular; LV $mass_i$ = left ventricular mass indexed; LVEF = left ventricular ejection fraction; $LVEDV_i$ = left ventricular end-diastolic volume indexed; $LVESV_i$ = left ventricular end-systolic volume indexed; MAPSE = mitral annular plane systolic excursion; MCF = myocardial contraction fraction; RA $area_i$ = right atrial area indexed; RV = right ventricular; RVEF = right ventricular ejection fraction; SV_i = stroke volume indexed; TAPSE = tricuspid annular plane systolic excursion; other abbreviations as in Table 1.

Survival was evaluated with Cox proportional hazards regression analysis, providing estimated hazard ratios with 95% confidence intervals (CIs) and Kaplan-Meier curves. The 11 echocardiography and CMR variables along with heart rate at the time of CMR study were first explored with simple Cox regression analysis. The variables that were statistically significant predictors of outcome on simple Cox regression analysis were entered into a multivariable Cox proportional hazards analysis to determine which covariates were independent predictors of mortality. The relationships between candidate predictors were first explored with correlational analysis. Possible collinearity among candidate predictors was subsequently assessed using variance inflation factors with threshold equal to 5. Separate multivariable models were performed to exclude parameters that are derived from one another (e.g., LVEF and MCF both are derived from SV; MCF being derived from SV and myocardial mass). Thus, model A included indexed LV SV and mass (and excluded MCF and LVEF); model B included LVEF and LV mass (SV and MCF were excluded); and model C included MCF (SV, LV mass and LVEF were excluded). Subanalyses of the AL and ATTR amyloidosis patient cohorts were also performed. The Harrell C statistic was calculated for the different models.

RESULTS

STUDY POPULATION CHARACTERISTICS. Details of the 322 subjects are shown in Table 1. The TTR mutations in the 158 patients with definite cardiac ATTR amyloidosis were as follows: V122I, n = 30; T60A, n = 16; V30M, n = 3; E89K, n = 2; and E54G, D38Y, F44L, and I73V, n = 1 each. Of 20 patients with suspected

FIGURE 1 The Probability of Cardiac Structural and Functional Variables Being Abnormal Across the Spectrum of Cardiac Amyloid Burden (as Defined by ECV)

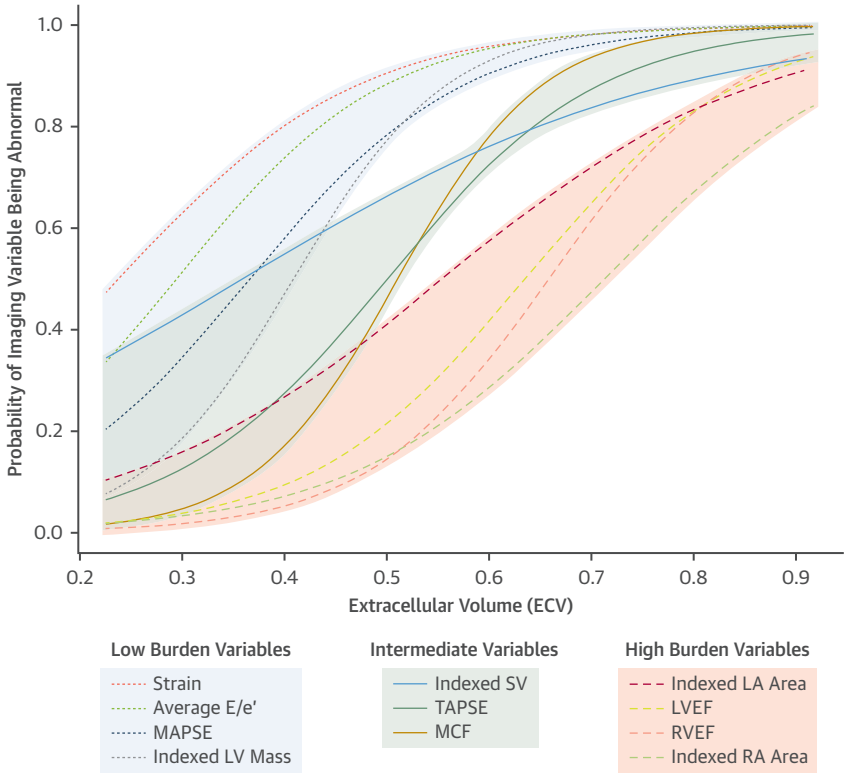

Variables can be categorized into 3 groups according to their likelihood of being abnormal: either predominantly at low or high burdens of cardiac infiltration, or with a progressively rising probability of being abnormal across the spectrum of myocardial amyloid burden (intermediate). ECV = extracellular volume; LA = left atrial; LV = left ventricular; LVEF = left ventricular ejection fraction; MAPSE = mitral annular plane systolic excursion; MCF = myocardial contraction fraction; RA = right atrial; RVEF = right ventricular ejection fraction; SV = stroke volume; TAPSE = tricuspid annular plane systolic excursion.

cardiac ATTR amyloidosis, the TTR mutations were as follows: S77Y, n = 3; V122I and V30M, n = 2 each; E54G, G47V, I84S, and I107F, n = 1 each. Of the 11 asymptomatic individuals with TTR mutations, 6 had TTR V30M, 4 had T60A, and 1 had S77Y. Patients with ATTR amyloidosis were older, had poorer renal function, and a higher prevalence of electrocardiographic conduction abnormalities. Twenty-three patients were excluded from ECV analysis due to significant renal impairment precluding gadolinium administration (n = 5) or due to constraints specific to the clinical circumstances (n = 18).

RELATIONSHIP BETWEEN NONINVASIVE FUNCTIONAL METRICS AND ECV. The ECV values in the 299 patients who underwent this assessment by CMR were divided into tertiles. Increasing myocardial amyloid burden across these ECV tertiles was associated with several structural and functional changes in both the AL and ATTR patient cohorts (Table 2): more severe diastolic dysfunction and worsening LGS by echocardiography; increased LV mass, increased biventricular end-systolic volumes, decreased biventricular EFs, decreased SV, and worsening biventricular longitudinal function. In ATTR, increasing ECV burden was also associated with increased biventricular end-diastolic volumes and increased biatrial areas.

When using ECV as a marker of cardiac infiltration burden, the CMR and echocardiography functional metrics can be grouped by the probability of becoming abnormal at low or high disease burdens or gradually across the spectrum of myocardial infiltration (Figure 1). Indexed LV mass and MAPSE by CMR along with LGS and E/e′ by echocardiography have a high probability of being abnormal at low cardiac amyloid burdens. Conversely, biventricular EFs and biatrial areas become abnormal at higher burdens of

cardiac infiltration. The probabilities of MCF, TAPSE, and indexed SV becoming abnormal increase gradually across the spectrum of ECVs.

NONINVASIVE FUNCTIONAL AND STRUCTURAL METRICS AND PROGNOSIS. Ninety patients (28%) died during a median follow-up period of 22 months (interquartile range: 10 to 38 months). All of the imaging metrics studied except for heart rate were predictive of mortality on simple Cox regression analysis (Table 3). Only CMR-derived TAPSE (hazard ratio [HR]: 1.46; 95% CI: 1.16 to 1.85; $p < 0.01$) and indexed SV (HR: 1.24; 95% CI: 1.04 to 1.48; $p < 0.05$) remained independently predictive of mortality in a multivariable Cox model adjusted for age and sex (Table 4, Figure 2). Harrell's C-statistic for this model was 0.73. When performing different multivariable models to avoid statistical coupling of the entered variables, TAPSE remained independently predictive of mortality (Table 4). The marked differences in significance levels from univariable to multivariable analyses are partly due to the correlation among covariates (Online Table 1). However, exploring variance inflation factors and using a threshold equal to 5 found no evidence of collinearity among the parameters entered into the multivariable analyses.

Functional parameters by echocardiography and CMR were also entered into multivariable Cox regression models for AL and ATTR patient subgroups (Online Tables 2 and 3, respectively). In ATTR cardiac amyloidosis, TAPSE was consistently significantly associated with mortality (HR: 1.53; 95% CI: 1.08 to 2.16; $p < 0.05$; Harrell's C-statistic 0.729). Three metrics were consistently significantly associated with mortality in AL cardiac amyloidosis, namely, LA area indexed (HR: 1.53; 95% CI: 1.12 to 2.09; $p < 0.01$), SV indexed (HR: 1.37; 95% CI: 1.03 to 1.83; $p < 0.05$) and TAPSE (HR: 1.54; 95% CI: 1.08 to 2.18; $p < 0.05$; Harrell's C-statistic 0.797).

TABLE 3 Simple Cox Regression Analysis of Risk of Death in the Overall Population

	Univariable	
	HR (95% CI)	p Value
Heart rate, beats/min	1.01 (0.99–1.02)	0.608
E/e' each 1-U increment	1.03 (1.01–1.05)	0.005*
LV LGS, each 2% decrement	1.24 (1.13–1.36)	0.000004†
LV mass indexed, each 10-g/m^2 increment	1.07 (1.02–1.13)	0.009*
LA area indexed, each 1.8-cm^2/m^2 increment	1.25 (1.10–1.41)	0.001*
RA area indexed, each 1.8-cm^2/m^2 increment	1.18 (1.07–1.29)	0.001*
LVEF, each 3% decrement	1.12 (1.07–1.17)	5.0×10^{-7}†
RVEF, each 3% decrement	1.14 (1.08–1.19)	1.9×10^{-7}†
SVi, each 5-ml/m^2 decrement	1.40 (1.24–1.57)	4.8×10^{-8}†
MAPSE, each 2.2-mm decrement	1.43 (1.23–1.66)	0.000002†
TAPSE, each 3.6-mm decrement	1.70 (1.45–2.00)	1.3×10^{-10}†
MCF, each 10% decrement	1.55 (1.32–1.81)	3.5×10^{-8}†

*$p < 0.01$. †$p < 0.001$.
CI = confidence interval; HR = hazard ratio; other abbreviations as in Table 2.

RELATIONSHIP BETWEEN RV LGE AND TAPSE. Evidence of RV cardiac amyloidosis involvement, defined by the presence of RV LGE, was determined given the significant association of TAPSE with mortality. An increasing prevalence of RV LGE was observed in both AL and ATTR patient cohorts with increasing amyloid burden measured by ECV (Table 2). Two hundred twenty-nine subjects (70%; 73 [63%] of AL amyloidosis patients, 156 [85%] of ATTR subjects including mutation carriers) on LGE assessment had evidence of RV cardiac amyloidosis, with

TABLE 4 Multivariable Cox Regression Analysis of Risk of Death in the Overall Population

	Model A		Model B		Model C	
	HR (95% CI)	p Value	HR (95% CI)	p Value	HR (95% CI)	p Value
E/e' each 1-U increment	1.02 (0.98–1.05)	0.40	1.02 (0.98–1.06)	0.33	1.00 (0.96–1.04)	0.99
LV LGS, each 2% decrement	1.02 (0.89–1.18)	0.76	1.03 (0.89–1.19)	0.69	1.08 (0.94–1.25)	0.27
LV mass index, each 10-g/m^2 increment	0.97 (0.90–1.05)	0.49	0.95 (0.88–1.02)	0.16	–	–
LA area index, each 1.8-cm^2/m^2 increment	1.18 (0.99–1.40)	0.060	1.11 (0.95–1.30)	0.20	1.08 (0.93–1.26)	0.32
RA area index, each 1.8-cm^2/m^2 increment	1.02 (0.90–1.16)	0.71	1.02 (0.89–1.16)	0.81	1.02 (0.90–1.15)	0.79
LVEF, each 3% decrement	–	–	1.04 (0.96–1.14)	0.33	–	–
RVEF, each 3% decrement	1.02 (0.95–1.10)	0.60	1.00 (0.91–1.09)	0.93	1.02 (0.95–1.09)	0.60
SVi, each 5-ml/m^2 decrement	1.24 (1.04–1.48)	0.019*	–	–	–	–
MAPSE, each 2.2-mm decrement	1.00 (0.82–1.22)	0.99	1.03 (0.85–1.26)	0.74	1.02 (0.84–1.24)	0.84
TAPSE, each 3.6-mm decrement	1.46 (1.16–1.85)	0.0014†	1.55 (1.23–1.96)	0.00026‡	1.48 (1.17–1.87)	0.0012†
MCF, each 10% decrement	–	–	–	–	1.25 (1.00–1.57)	0.053
C-statistic	0.729 (0.639, 0.819)		0.724 (0.634, 0.814)		0.725 (0.635, 0.815)	

*$p < 0.05$. †$p < 0.01$. ‡$p < 0.001$.
Abbreviations as in Tables 2 and 3.

FIGURE 2 Kaplan-Meier Curves

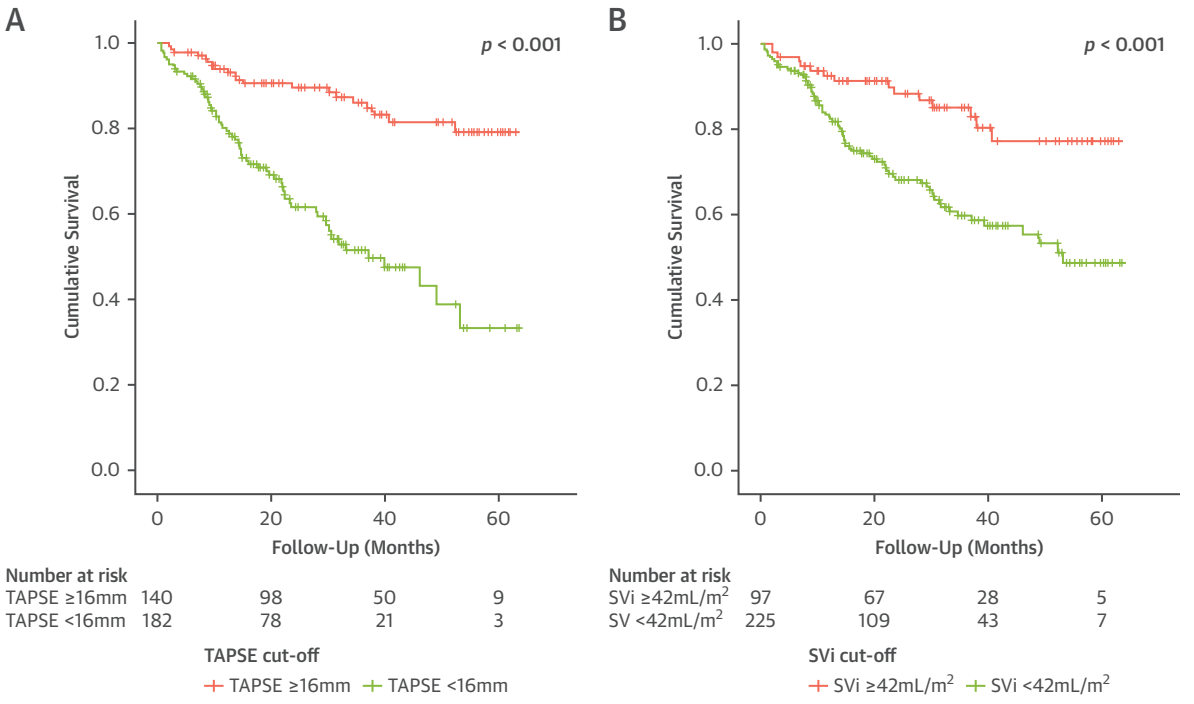

Kaplan-Meier curves for TAPSE **(A)** and indexed stroke volume **(B).** Kaplan-Meier curves displaying event-free survival in all patients according to **(A)** CMR-derived TAPSE ≥16 mm or <16 mm and **(B)** indexed stroke volume ≥42 ml/m^2 or <42 ml/m^2. CMR = cardiac magnetic resonance; SVi = indexed stroke volume; other abbreviations as in Figure 1.

corresponding significantly lower TAPSE across all patient subgroups (Table 5).

DISCUSSION

In this study, we comprehensively describe the structural and functional cardiac abnormalities associated with cardiac infiltration using commonly used CMR and echocardiography parameters. To our knowledge, this is also the largest study to identify the strongest prognostic, structural, and functional cardiac imaging metrics in amyloidosis.

EF is a ubiquitous marker conventionally used to describe cardiac function, especially in the setting of heart failure. However, symptoms and signs of cardiac decompensation are known to commonly precede significant deterioration in EF in amyloidosis (25). Our data confirm that biventricular EFs tend to be preserved up until higher burdens of cardiac infiltration, with abnormalities in biatrial size also reflecting the most advanced stages of the disease process. Echocardiography and CMR functional metrics can be divided into a cascade of 3 groups that become abnormal sequentially with increasing cardiac amyloid burden as assessed by ECV quantification. Variables more likely to become abnormal at low levels of cardiac infiltration reflect impairment of LV diastolic function and LV longitudinal dysfunction, both of which are not accounted for by global EF. Despite E/e′ and myocardial mass being generated by different imaging modalities (echocardiography and CMR, respectively), they become abnormal in parallel across increasing amyloid deposition. This reflects the close relationship between amyloid burden and diastolic dysfunction, particularly in early cardiac involvement. LGS and MAPSE also tend to become abnormal at the lower end of the ECV spectrum. Both of these parameters reflect longitudinal impairment, an early marker of systolic dysfunction that is not accounted for by global EF (26). This is especially pertinent in cardiac amyloidosis due to infiltration starting in the subendocardium, predominantly consisting of longitudinal fibers.

LV SV, MCF, and TAPSE constitute the intermediate group of variables with a probability of being abnormal that rises progressively across the spectrum

TABLE 5 Relationship Between RV LGE and TAPSE in Patients With AL and ATTR Amyloidosis

	All Subjects (n = 299)		AL (n = 116)		ATTR (n = 183)	
	RV LGE Present	RV LGE Absent	RV LGE Present	RV LGE Absent	RV LGE Present	RV LGE Absent
N (%)	229 (77)	70 (23)*	73 (63)	43 (37)†	156 (85)	27 (15)*
TAPSE	12 (9–16)	21 (17–24)*	14 (10–19)	21 (17–24)*	12 (9–15)	20 (18–25)*

Values are n (%) or median (Q1–Q3). *$p < 0.001$ and †$p < 0.01$ for differences between RV LGE positive and negative groups.
Abbreviations as in Tables 1 and 2.

of increasing amyloid burden. In contrast to EF, SV has a high probability of being abnormal in the earlier stages of cardiac amyloid infiltration. This could be due to the initial increase in myocardial mass conferring a smaller end-diastolic cavity volume. However, the likelihood of SV being abnormal then continues to rise with increasing levels of amyloid burden, possibly reflecting the later development of impaired radial function with progression from subendocardial to transmural amyloid deposition. Thus, abnormal SV is likely to represent a composite signal of diastolic dysfunction at low burdens of cardiac amyloidosis and systolic contractile impairment at higher burdens of cardiac infiltration. The progressively increasing likelihood of MCF becoming abnormal with rising ECV reflects the behaviors of the variables from which it is derived, namely, SV and myocardial mass. The likelihood of TAPSE being abnormal also increases gradually across the spectrum of rising myocardial infiltration, whereas global RVEF becomes abnormal at high burdens of cardiac involvement. This difference is likely to be due to TAPSE reflecting infiltration of subendocardial longitudinal fibers in the earlier stages of the disease, whereas radial dysfunction and congestive heart failure manifest late in the natural history of the disease.

Interestingly, TAPSE and indexed SV were the only prognostic markers for mortality in the multivariable model of all amyloidosis patients. TAPSE was the most statistically significant independent marker of prognosis, and was the only prognostic marker common to the subgroup analyses of both AL and ATTR patient cohorts. RV dysfunction is common in cardiac amyloidosis (7). Furthermore, RV failure is a well-documented independent predictor of prognosis in patients with primary left heart failure (27–29). However, direct RV subendocardial infiltration is likely to be the principal reason behind the prognostic importance of TAPSE in amyloidosis, rather than RV dysfunction as a consequence of LV impairment. This is evidenced by the high prevalence of RV LGE in both AL and ATTR patient cohorts, and explains why TAPSE rather than RVEF is the key prognostic marker in amyloidosis overall. This is also in contrast to RV pressure-overload states, whereby radial rather than longitudinal contraction more closely reflects global RV function, with global RVEF being a consistently strong predictor of outcome (30–32). The main finding on subgroup analysis of the AL and ATTR patient cohorts was that LA area was an additional significant prognostic marker in the AL patient cohort, consistent with previous echocardiography studies in AL amyloidosis (33,34). Thus, LA dilatation could represent a structural marker of more advanced disease.

STUDY LIMITATIONS. The study was retrospective, with approximately one-quarter of patients excluded due to incomplete data acquisition. However, the number of events in the remaining 322 patients is sufficient for the multivariable analyses. The study design was also cross-sectional, with patients scanned at different stages of presentation and treatment. This might include chemotherapy for patients with AL amyloidosis, with some agents having known cardiotoxic side effects that could also influence the measurement of the variables under investigation. Furthermore, the assessment of disease progression would require serial assessments of these measures in the same individuals over time. Patients with ATTR amyloidosis might be more likely to present at later stages of cardiac infiltration when symptoms of cardiac failure are manifest, reflected by the smallest proportion of ATTR patients being in the lowest ECV tertile (19%). This might affect the changes observed in cardiac markers at low amyloid burdens in this cohort. The inclusion of 20 suspected ATTR cases and 11 asymptomatic TTR gene mutation carriers, all of whom potentially may have subclinical or very early disease, might at least partly offset this limitation. Conversely, the largest proportion of AL patients were in the lowest ECV tertile (62%), again likely representing the manner of clinical presentation. Overall, 23 patients did not have ECV measured either due to significant renal dysfunction or clinical constraints at the time of scanning. Patients with implanted cardiac defibrillators or permanent pacemakers were also

excluded from CMR study. Given that these patients are known to have an adverse prognosis, their exclusion could affect the survival analysis. However, these limitations all reflect real-world practice and the presentation of patients for clinical evaluation. The simple logistic regression analysis dichotomized each variable as abnormal or normal according to predefined cut-off values derived from healthy populations, rather than from patient populations with cardiac amyloidosis. Although these cut-off values from a normal population would have less direct clinical relevance to a cardiac amyloidosis predominant population, our aim was to describe the behavioral changes in cardiac markers across the spectrum of cardiac infiltration rather than specify the diagnostic threshold of the cut-off values themselves. Finally, cardiac biopsy was performed in a minority of patients, but the entire cohort underwent comprehensive composite noninvasive evaluation including DPD scanning. This is our routine clinical protocol, and is known to deliver high diagnostic accuracy.

CONCLUSIONS

In the multimodality cardiac imaging assessment of patients with amyloidosis, TAPSE and LV indexed SV measured by CMR are the most powerful prognostic cardiac functional parameters. They are standard and simply obtained measures, with a likelihood of being abnormal that increases with rising cardiac amyloid burden.

ADDRESS FOR CORRESPONDENCE: Dr. Marianna Fontana, Centre for Amyloidosis & Acute Phase Proteins, Division of Medicine (Royal Free Campus), University College London, Rowland Hill Street, London NW3 2PF, United Kingdom. E-mail: m.fontana@ucl.ac.uk.

PERSPECTIVES

COMPETENCY IN MEDICAL KNOWLEDGE: Cardiac involvement in amyloidosis is the main determinant of prognosis. The behavior and prognostic importance of common cardiac functional and structural markers by echocardiography and CMR have been evaluated in a cross-sectional study of patients with systemic amyloidosis. Both TAPSE and indexed SV have an increasing likelihood of becoming abnormal with rising cardiac amyloid burden, and are independently prognostic in systemic amyloidosis.

TRANSLATIONAL OUTLOOK: The behavior of cardiac structural and functional parameters can be interpreted in relation to the pathophysiology of amyloidosis across the spectrum of cardiac disease burden. Prospective clinical studies of serial cardiac imaging assessments are required to evaluate the progression of structural and functional cardiac measures with increasing myocardial amyloid burden.

REFERENCES

1. Wechalekar AD, Gillmore JD, Hawkins PN. Systemic amyloidosis. Lancet 2016;387:2641–54.

2. Fontana M, Pica S, Reant P, et al. Prognostic value of late gadolinium enhancement cardiovascular magnetic resonance in cardiac amyloidosis. Circulation 2015;132:1570–9.

3. Quarta CC, Solomon SD, Uraizee I, et al. Left ventricular structure and function in transthyretin-related versus light-chain cardiac amyloidosis. Circulation 2014;129:1840–9.

4. Falk RH, Comenzo RL, Skinner M. The systemic amyloidoses. N Engl J Med 1997;337:898–909.

5. Rapezzi C, Merlini G, Quarta CC, et al. Systemic cardiac amyloidoses: disease profiles and clinical courses of the 3 main types. Circulation 2009;120:1203–12.

6. Bellavia D, Pellikka PA, Dispenzieri A, et al. Comparison of right ventricular longitudinal strain imaging, tricuspid annular plane systolic excursion, and cardiac biomarkers for early diagnosis of cardiac involvement and risk stratification in primary systematic (AL) amyloidosis: a 5-year cohort study. Eur Heart J Cardiovasc Imaging 2012;13:680–9.

7. Bodez D, Ternacle J, Guellich A, et al. Prognostic value of right ventricular systolic function in cardiac amyloidosis. Amyloid 2016:1–10.

8. Cappelli F, Porciani MC, Bergesio F, et al. Right ventricular function in AL amyloidosis: characteristics and prognostic implication. Eur Heart J Cardiovasc Imaging 2012;13:416–22.

9. Cueto-Garcia L, Reeder GS, Kyle RA, et al. Echocardiographic findings in systemic amyloidosis: spectrum of cardiac involvement and relation to survival. J Am Coll Cardiol 1985;6:737–43.

10. Klein AL, Hatle LK, Taliercio CP, et al. Prognostic significance of Doppler measures of diastolic function in cardiac amyloidosis. A Doppler echocardiography study. Circulation 1991;83:808–16.

11. Koyama J, Falk RH. Prognostic significance of strain Doppler imaging in light-chain amyloidosis. J Am Coll Cardiol Img 2010;3:333–42.

12. Ternacle J, Bodez D, Guellich A, et al. Causes and consequences of longitudinal LV dysfunction assessed by 2D strain echocardiography in cardiac amyloidosis. J Am Coll Cardiol Img 2016;9:126–38.

13. Gillmore JD, Maurer MS, Falk RH, et al. Nonbiopsy diagnosis of cardiac transthyretin amyloidosis. Circulation 2016;133:2404–12.

14. Martinez-Naharro A, Treibel TA, Abdel-Gadir A, et al. Magnetic resonance in transthyretin cardiac amyloidosis. J Am Coll Cardiol 2017;70:466–77.

15. Lang RM, Bierig M, Devereux RB, et al. Recommendations for chamber quantification. Eur J Echocardiogr 2006;7:79–108.

16. Gottdiener JS, Bednarz J, Devereux R, et al. American Society of Echocardiography recommendations for use of echocardiography in clinical trials. J Am Soc Echocardiogr 2004;17:1086–119.

17. Nagueh SF, Appleton CP, Gillebert TC, et al. Recommendations for the evaluation of left ventricular diastolic function by echocardiography. J Am Soc Echocardiogr 2009;22:107–33.

18. Fontana M, White SK, Banypersad SM, et al. Comparison of T1 mapping techniques for ECV quantification. Histological validation and reproducibility of ShMOLLI versus mutlibreath-hold T1 quantification equilibrium contrast CMR. J Cardiovasc Magn Reson 2012;14:88.

19. White SK, Sado DM, Fontana M, et al. T1 mapping for myocardial extracellular volume measurement by CMR: bolus only versus primed infusion technique. J Am Coll Cardiol Img 2013;6:955–62.

20. Tendler A, Helmke S, Teruya S, Alvarez J, Maurer MS. The myocardial contraction fraction is superior to ejection fraction in predicting survival in patients with AL cardiac amyloidosis. Amyloid 2015;22:61–6.

21. Nagueh SF, Smiseth OA, Appleton CP, et al. Recommendations for the evaluation of left ventricular diastolic function by echocardiography: an update from the American Society of Echocardiography and the European Association of Cardiovascular Imaging. J Am Soc Echocardiogr 2016;29:277–314.

22. Kawel-Boehm N, Maceira A, Valsangiacomo-Buechel ER, et al. Normal values for cardiovascular magnetic resonance in adults and children. J Cardiovasc Magn Reson 2015;17:29.

23. Lang RM, Badano LP, Mor-Avi V, et al. Recommendations for cardiac chamber quantification by echocardiography in adults: an update from the American Society of Echocardiography and the European Association of Cardiovascular Imaging. J Am Soc Echocardiogr 2015;28:1–39 e14.

24. Akwo E. Myocardial contraction fraction, diabetes and heart failure: the multi ethnic study of atherosclerosis. A thesis submitted to the graduate faculty of Wake Forest University Graduate School Of Arts And Sciences; August 2012. Available at: https://wakespace.lib.wfu.edu/bitstream/handle/10339/37433/Akwo_wfu_0248M_10329.pdf. Accessed February 1, 2018.

25. Austin BA, Duffy B, Tan C, Rodriguez ER, Starling RC, Desai MY. Comparison of functional status, electrocardiographic, and echocardiographic parameters to mortality in endomyocardial-biopsy proven cardiac amyloidosis. Am J Cardiol 2009;103:1429–33.

26. Koyama J, Ray-Sequin PA, Falk RH. Longitudinal myocardial function assessed by tissue velocity, strain, and strain rate tissue Doppler echocardiography in patients with AL (primary) cardiac amyloidosis. Circulation 2003;107:2446–52.

27. de Groote P, Millaire A, Foucher-Hossein C, et al. Right ventricular ejection fraction is an independent predictor of survival in patients with moderate heart failure. J Am Coll Cardiol 1998;32:948–54.

28. Ghio S, Gavazzi A, Campana C, et al. Independent and additive prognostic value of right ventricular systolic function and pulmonary artery pressure in patients with chronic heart failure. J Am Coll Cardiol 2001;37:183–8.

29. Sun JP, James KB, Yang XS, et al. Comparison of mortality rates and progression of left ventricular dysfunction in patients with idiopathic dilated cardiomyopathy and dilated versus nondilated right ventricular cavities. Am J Cardiol 1997;80:1583–7.

30. Kind T, Mauritz GJ, Marcus JT, van de Veerdonk M, Westerhof N, Vonk-Noordegraaf A. Right ventricular ejection fraction is better reflected by transverse rather than longitudinal wall motion in pulmonary hypertension. J Cardiovasc Magn Reson 2010;12:35.

31. Moledina S, Pandya B, Bartsota M, et al. Prognostic significance of cardiac magnetic resonance imaging in children with pulmonary hypertension. Circ Cardiovasc Imaging 2013;6:407–14.

32. van Wolferen SA, Marcus JT, Boonstra A, et al. Prognostic value of right ventricular mass, volume, and function in idiopathic pulmonary arterial hypertension. Eur Heart J 2007;28:1250–7.

33. Mohty D, Pibarot P, Dumesnil JG, et al. Left atrial size is an independent predictor of overall survival in patients with primary systemic amyloidosis. Arch Cardiovasc Dis 2011;104:611–8.

34. Zhao L, Tian Z, Fang Q. Risk factors and prognostic role of left atrial enlargement in patients with cardiac light-chain amyloidosis. Am J Med Sci 2016;351:271–8.

KEY WORDS amyloidosis, CMR, echocardiography, function, prognosis

APPENDIX For supplemental tables, please see the online version of this article.